son, in *Emerging Lithographic Technologies III* (Ed: Y. Vladimirsky), SPIE, Bellingham, WA **1999**, p. 379.
[9] R. Maboudian, W. R. Ashurst, C. Carraro, *Sens. Actuators, A* **2000**, *82*, 2193.
[10] O. Azzaroni, P. L. Schilardi, R. C. Salvarezza, R. Gago, L. Vázquez, *Appl. Phys. Lett.* **2003**, *82*, 457.
[11] P. L. Schilardi, O. Azzaroni, R. C. Salvarezza, *Langmuir* **2001**, *17*, 2748.
[12] O. Azzaroni, P. L. Schilardi., R. C. Salvarezza, *Appl. Phys. Lett.* **2002**, *80*, 1061.
[13] B. Brezger, T. H. Schulze, U. Drodofsky, J. Stuhler, S. Nowak, T. Pfau, J. Mlynek, *J. Vac. Sci. Technol. B* **1997**, *15*, 2905.
[14] S. Rusponi, G. Constantini, F. Buatier de Mongeot, C. Boragno, U. Valbusa, *Appl. Phys. Lett.* **1999**, *75*, 3318.
[15] J. J. McClelland, R. E. Scholten, E. C. Palm, R. J. Celotta, *Science* **1993**, *262*, 877.
[16] R. Gago, L. Vázquez, R. Cuerno, M. Varela, C. Ballesteros, J. M. Albella, *Appl. Phys. Lett.* **2001**, *78*, 3316.
[17] H. Ron, H. Cohen, S. Matlis, I. Rubinstein, *J. Phys. Chem. B* **1998**, *102*, 9861.
[18] O. Azzaroni, M. E. Vela, M. Fonticelli, G. Benítez, B. Blum, P. Carro, R. C. Salvarezza, *J. Phys .Chem. B*, **2003**, *107*, 13 446.
[19] H. Masuda, K. Fukuda, *Science* **1995**, *268*, 1466.
[20] B. Michel, A. Bernard, A. Bietsch, E. Delamarche, M. Geissler, D. Juncker, H. Kind, J. P. Renault, H. E. Rothuizen, H. Schmid, P. Schmidt-Winkel, R. Stutz, H. Wolf, *IBM J. Res. Dev.* **2001**, *45*, 697.
[21] M. J. Tarlov, *Langmuir* **1992**, *8*, 80.
[22] F. Schreiber, *Prog. Surf. Sci.* **2000**, *65*, 151.
[23] A. Ulman, *Chem. Rev.* **1996**, *96*, 1533.
[24] O. Azzaroni, M. E. Vela, G. Andreasen, P. Carro, R. C. Salvarezza, *J. Phys. Chem. B* **2002**, *106*, 12 267.
[25] H. Hagenström, M. A. Schneeweiss, D. M. Kolb, *Langmuir* **1999**, *15*, 2435.
[26] O. Azzaroni, P. L. Schilardi, R. C. Salvarezza, *Electrochim. Acta* **2003**, *48*, 3107.
[27] M. Epple, A. M. Bittner, K. Kuhnke, K. Kern, W.-Q. Zheng, A. Tadjeddine, *Langmuir* **2002**, *18*, 773.
[28] O. Cavalleri, H. Kind, A. M. Bittner, K. Kern, *Langmuir* **1998**, *14*, 7292.
[29] A. Hooper, G. L. Fisher, K. Konstadinidis, D. Jung, H. Nguyen, R. Opila, R. W. Collins, N. Winograd, D. L. Allara, *J. Am. Chem. Soc.* **1999**, *121*, 8052.
[30] A. M. Sondag-Huethorst, L. G. J. Fokkink, *Langmuir* **1995**, *11*, 4823.
[31] S. Facsko, T. Dekorski, C. Koerdt, C. Trappe, H. Kurz, A. Vogt, H. L. Hartnagel, *Science* **1999**, *285*, 1551.
[32] S. Aggarwal, A. P. Monga, S. R. Perusse, R. Ramesh, V. Ballarotto, E. D. Williams, B. R. Chalamala, Y. Wei, R. H. Reuss, *Science* **2000**, *287*, 2235.
[33] L. E. Davis, N. C. MacDonald, P. W. Palmberg, G. E. Riachy, R. E. Weber, *Handbook of Auger Electron Spectroscopy*, 2nd ed., Physical Electronics, Eden Prairie, MN **1976**.
[34] Y. L. Loo, R. W. Willett, K. Baldwin, J. A. Rogers, *J. Am. Chem. Soc.* **2002**, *124*, 7654.
[35] C. Kim, M. Shtein, S. R. Forrest, *Appl. Phys. Lett.* **2002**, *80*, 4051.
[36] J. Zaumseil, M. A. Meitl, J. W. P. Hsu, B. Acharya, K. W. Baldwin, Y.-L. Loo, J. A. Rogers, *Nano Lett.* **2003**, *3*, 1223.
[37] H. Schmid, H. Wolf, R. Allenspach, H. Riel, S. Karg, B. Michel, E. Delamarche, *Adv. Funct. Mater.* **2003**, *13*, 145.
[38] *Applications of Atomic Force Microscopy in Optical Disc Technology*, Digital Instruments Applications Notes. http://www.di.com
[39] D. M. Kolb, R. Ulman, T. Will, *Science* **1997**, *275*, 1097.
[40] P. Vettiger, J. Brugger, M. Despont, U. Drechsler, U. Dürig, W. Häberle, M. Lutwyche, H. Rothuizen, R. Stutz, R. Widmer, G. Binnig, *Microelectron. Eng.* **1999**, *46*, 11.
[41] D. K. Schwartz, *Annu. Rev. Phys. Chem.* **2001**, *52*, 107.

Regular Arrays of Copper Wires Formed by Template-Assisted Electrodeposition**

By *Mingzhe Zhang*, *Steven Lenhert*, *Mu Wang*,* *Lifeng Chi*,* *Nan Lu*, *Harald Fuchs*, and *Naiben Ming*

Electrodeposition—or electroplating—has been intensively investigated in recent decades, as it is an important method for fabricating metallic thin films.[1] In recent years, much effort has been devoted to patterned electrodeposition,[2–5] which is expected to be a promising technique for fabricating micro-/nanostructures in a "bottom–up" fashion, and may have applications in future generations of microelectronics,[6] miniaturized sensors,[7] and microelectromechanical systems.[8,9] There are generally two ways to achieve patterned electrodeposition. In one scenario, the pattern is achieved via self-organization. For example, in an ultrathin electrolyte layer the electrodeposits may have a considerably low branching rate[4] and the branches may self-organize into regular arrays of metallic wires.[10] However, achieving a regular array over a large area by self-organization remains a technical challenge. An alternative method is template-assisted electrodeposition.[11] For example, with the help of ordered channels in anodized aluminum oxide, arrays of metallic nanowires can be fabricated,[12] however a large-area ordered template of anodized aluminum oxide is extremely difficult to prepare.[12] Therefore, the essential problem for patterned electrodeposition is to find an easy, cheap, and high-throughput way to generate ordered templates. Recently, it has been found that when monolayers are transferred onto a solid substrate, a regular striped pattern can be formed due to the wetting instabilities of the Langmuir film under low surface pressure.[13] In this way, a heterogeneously structured surface with periodic re-

[*] Prof. M. Wang, Dr. M. Zhang, Prof. N. B. Ming
National Laboratory of Solid State Microstructures
Nanjing University
Nanjing 210 093 (P.R. China)
E-mail: muwang@nju.edu.cn
[*] Dr. L. Chi, Dr. M. Zhang, S. Lenhert, Dr. N. Lu, Prof. H. Fuchs
Physikalisches Institut, Westfälische Wilhelms-University
D-48 149 Münster (Germany)
E-mail: chi@uni-muenster.de
Prof. M. Wang
International Center of Quantum Structures, Institute of Physics
Chinese Academy of Sciences
Beijing 100 080 (P.R. China)
Dr. L. Chi, S. Lenhert, Dr. N. Lu, Prof. H. Fuchs
Center for Nanotechnology (CeNTech)
Gievenbecker Weg 11, D-48 149 Münster (Germany)
[**] This work was funded by a German–Chinese cooperation program supported by the state of North Rhine–Westphalia. It was also supported by the Ministry of Science and Technology of China (Grant No. G1998061410) and the National Science Foundation of China (Grant Nos. 10374043 and 10021001).

 DOI: 10.1002/adma.200305577

ADVANCED MATERIALS

gions of alternating surface free energies can be achieved. In this communication, we report the electrodeposition of regular arrays of submicrometer-wide copper wires over a silicon substrate, with the help of a patterned Langmuir–Blodgett (LB) film. We show that the width of the wires is homogeneous, and both the width and the separation of the wires can be tuned by the template, across a range of 100 nm to more than 1 μm.

The substrate for electrodeposition was prepared in the following way. The silicon surface was first cleaned and oxidized with O_2 plasma, and then covered with monolayer-thick regular stripes of L-α-dipalmitoylphosphatidylcholine (DPPC) by the previously reported method.[13–15] In this way, alternating stripes of DPPC and silicon oxide were generated, as shown in Figures 1a,b. We have found that the widths of the DPPC stripes and the silicon dioxide channels depend on the experimental control parameters. The periodicity of the pattern was determined by the transfer speed, whereas the ratio of the width of the stripe to the width of the channel depended on the surface density of the Langmuir film during the transfer. Thereafter, the DPPC stripes were used as a mask, and 3-aminopropyltrimethoxysilane was silicized in the silicon dioxide channels (Fig. 1c). Ultrasonication and rinsing with chloroform removed the residual silane and DPPC stripes, thus achieving a template with alternating stripes of amine groups and silicon dioxide.[16] The regular amino stripes on the substrate were used as a template for depositing copper by the unique method of ultrathin electrochemical deposition.[4,10] The setup for electrodeposition is schematically shown in Figures 1e,f. In the electrodeposition experiment, the copper filaments developed from the cathode, following the aminosilane tracks on the substrate and growing towards the anode, as indicated in Figure 1e.

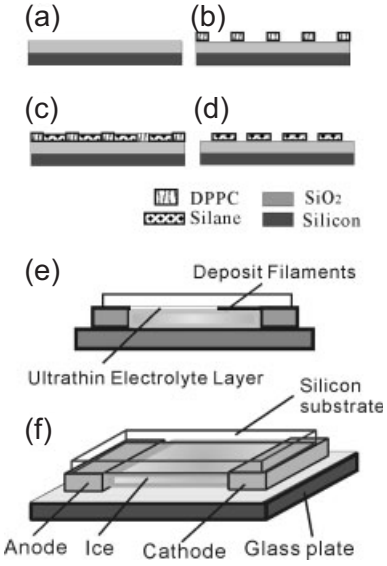

Figure 1. a–d) Schematic diagrams showing the procedure used to prepare the patterned substrate for electrodeposition. a) The surface of a silicon wafer is first oxidized. b) A periodic line pattern of DPPC is introduced on the substrate surface by pulling the LB film. c) Aminosilane molecules are self-assembled into the silicon dioxide channels. d) The DPPC stripes are removed; the aminosilane stripes remain. Copper crystallites will be nucleated on the aminosilane stripes. e,f) The side view and stereo view of the cell for electrodeposition. The surface with aminosilane contacts the electrolyte, on which the copper filaments will develop.

In our experiment, we applied a constant voltage across the electrodes. Figure 2a shows the copper wires generated at 2.0 V viewed by scanning electron microscopy (SEM). The wires were robustly deposited on the substrate. They are straight, equally spaced, and homogeneous in width. The height of the copper wires, according to our atomic force microscopy (AFM) measurements, is of the order of 50 nm when the control parameters were set as $C = 0.07$ M, where C is the concentration of $CuSO_4$, $V = 2.0$ V, pH 3.4, and $T = -4.2$ °C. Our experiments show that the height of the wires depended on the pH and the concentration of the electrolyte. At lower concentrations and lower pH, the height of the wires was lower. The largest area with strictly regular copper wire arrays that we achieved was about 200 μm × 200 μm, which could be improved by increasing the homogeneity of the ultrathin film of electrolyte. Figure 2b shows the very tips of the copper filaments grown on the substrate, which follow the templates on the substrate. Since the template structure is pre-designed and controllable, for each substrate we know the width of the stripes of aminosilane and width of the silicon oxide exactly. By checking the width of the copper filaments and the separa-

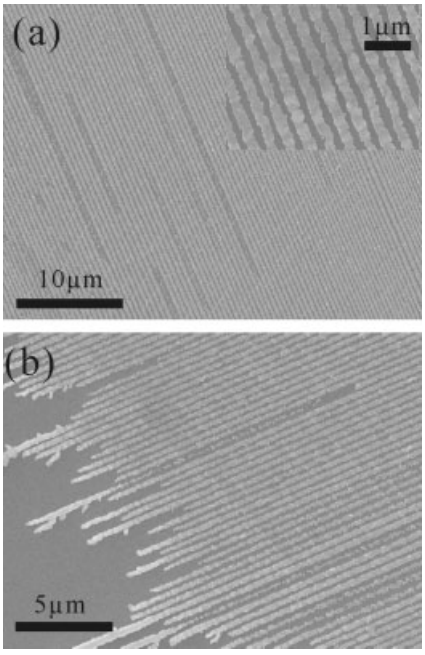

Figure 2. Scanning electron micrographs showing the copper wire arrays deposited on the patterned substrate. a) The copper wires are straight and homogeneous in width. b) The very front tips of the copper wires grown on the patterned substrate. The broadening of the tip is due to the residual growth of the copper crystallites when the power supply for electrodeposition is switched off.

tions between the copper filaments, we conclude that the copper covers the region terminated with aminosilane.

Figure 3 shows copper wires with different widths and inter-wire separations, which were achieved by using templates with different structures. One may also see in Figure 3 that the

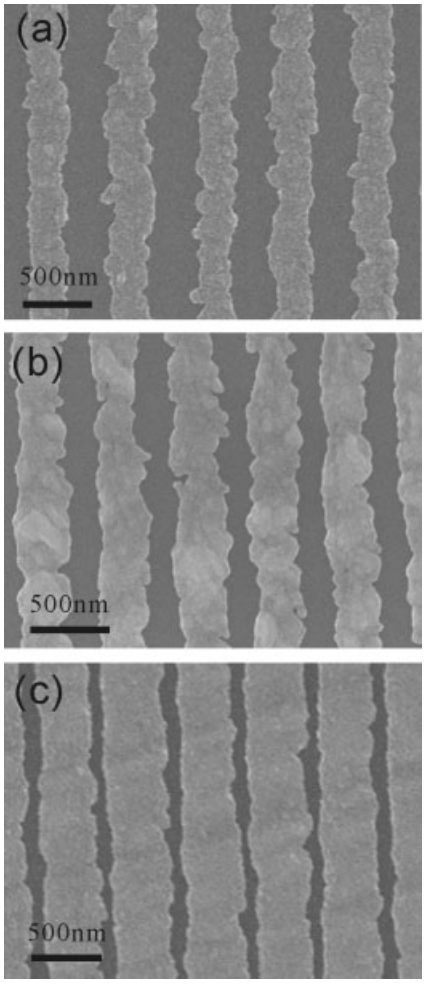

Figure 3. The ratio of the width of the copper wires to the width of the separation between neighboring wires was determined by the patterns on the template. The widths of the amino stripes and the silicon dioxide channels on the template are about: a) 200 nm and 200 nm; b) 300 nm and 200 nm; and c) 400 nm and 100 nm, respectively. Hence, the copper wires in these cases are about 200 nm, 300 nm, and 400 nm wide, accordingly. These micrographs also indicate that the copper wires are polycrystalline.

wires consist of small crystallites. The polycrystalline feature of the wires was confirmed by transmission electron microscopy (TEM). Figure 4a displays the diffraction contrast micrograph of the wire, where the separated grains can be easily identified. As indicated in the diffraction pattern, in addition to the dominant, strong diffractions of copper, some faint dots (rings) corresponding to the diffraction of Cu_2O can be recognized. Since both copper and cuprous oxide are polycrystalline, and the orientations of the crystallites are random, we may compare the concentrations of the crystallites of copper

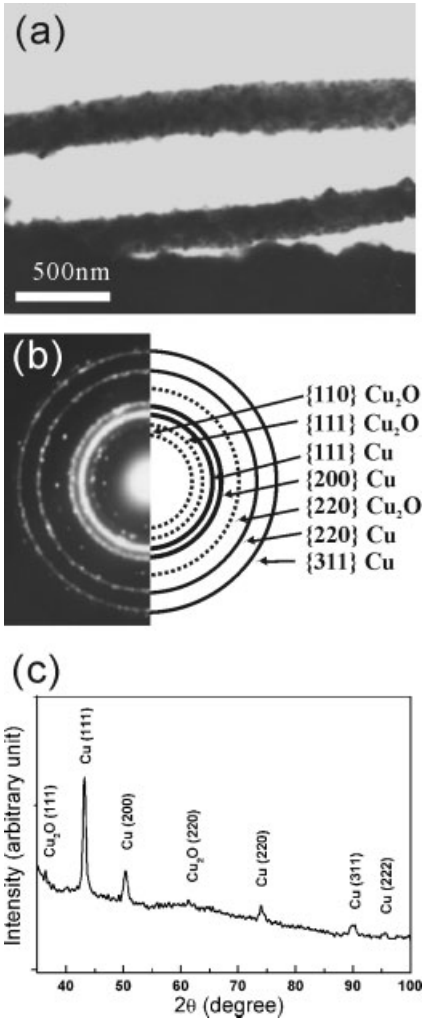

Figure 4. a) The transmission electron micrograph of the copper wires (the dark filaments). Some individual crystallites can be identified in the copper wire. b) The electron diffraction of the copper wire, which confirms that the wire is polycrystalline. The diffraction rings can be indexed. In addition to the diffraction of copper crystallites, faint diffraction spots/rings originating from Cu_2O can be identified. c) The X-ray diffraction pattern of the electrodeposits.

and the crystallites of cuprous oxide by comparing the intensity of the diffraction rings.[4,10] According to the standard diffraction database, the intensities of (200) of copper and (111) of cuprous oxide should be similar if their amount is the same. Yet Figure 4b indicates that the ring corresponding to (111) of cuprous oxide is much fainter than that of (200) of copper. We therefore conclude that the concentration of Cu_2O crystallite in the wire is very low. Figure 4c shows the X-ray diffraction pattern of the electrodeposits. Since the electrodeposits are very thin, the overall diffraction signal is weak. Yet, from Figure 4c, one may still see that the diffraction from Cu_2O is much weaker than that from copper, indicating the low concentration of Cu_2O crystallites in the electrodeposits.

Two factors are essential for the formation of the arrays of copper wire on the substrate. One is that the copper crystallites should be nucleated on the substrate and form a robust

ADVANCED MATERIALS

metal deposit, instead of generating an aggregate floating in the aqueous solutions;[17–19] the second factor is that the electrodeposits should follow the patterns on the substrate. The nucleation barrier for copper electrocrystallization is the key to fulfilling these requirements. In electrocrystallization, the nucleus should be electrically connected to the cathode. As we demonstrated previously, the concave corner of the copper deposit and the substrate is the most favorable site for nucleation when the thickness of the electrolyte layer becomes sufficiently thin.[20] Now we consider nucleation of the copper crystallite on the substrate on Sites 1,2, as shown in Figure 5. On Site 1, the nucleus contacts the grown copper wire and the aminosilane stripe. On Site 2, the nucleus contacts the copper

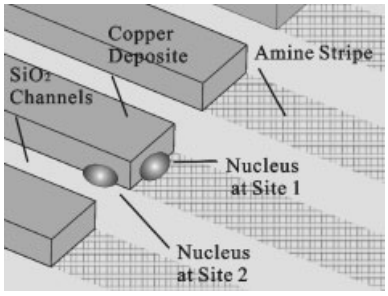

Figure 5. A schematic diagram showing the possible sites of nucleation in electrodeposition. On Site 1, the nucleus contacts the copper wire and the aminosilane stripe, whereas on Site 2 the nucleus contacts the copper wire and the silicon dioxide. The nucleation barriers on these two sites are different.

wire and the silicon dioxide substrate. It is known that in aqueous solution the interfacial energy of amino-terminated surfaces (stripes) is about 2.5 $N\,m^{-1}$[21] and that of silicon dioxide (channels) is of the order of 1.1 $N\,m^{-1}$.[22] Naturally, one may expect that the decrease in the free energy by forming a nucleus on Site 1, ΔG_1^*, is larger than that on Site 2, ΔG_2^*. This means that formation of copper crystallites along the stripes of aminosilane is thermodynamically favored, and thus the wires, as shown in Figure 2, can be formed.

The key challenges in producing desired nanostructures over a large application area are the simplicity, low cost, and high throughput of the fabrication method. The template-assisted electrodeposition reported in this communication demonstrates that we have found a promising way of generating arrays of straight copper wires on a solid substrate. The width of the copper wires, and the separation between them, can be controlled by the template. We need to emphasize that this method is not limited to copper electrodeposition. As a matter of fact, by selecting proper organic functionalized molecules, one may generate a patterned substrate with a specific distribution of surface free energy, on which metal crystallites will be selectively deposited. Therefore, this method can be applied to the fabrication of micro- or nanostructures of other metals. We expect that the direct and alternating electric properties of these metallic structures may have potential applications in microelectronics and optoelectronics.

Experimental

Langmuir–Blodgett (LB) films were prepared with commercial Langmuir–Blodgett film balances (KSV 3000 and NIMA 6100). The trough was filled with ultrapure water (Millipore, resistivity 18.2 MΩ cm). L-α-Dipalmitoylphosphatidylcholine (DPPC) (Fluka) was dissolved in chloroform (HPLC, Baker) and its concentration was 2.0 mM. Silicon substrates (WaterNet Co., orientation [100]) were cleaned and oxidized in an O_2 plasma (Templa System 100-E plasma system) [16]. The oxidized silicon surface was hydrophilic. The DPPC monolayer was kept in a low-pressure state (2.0–3.0 $mN\,m^{-1}$) at a constant temperature (25 °C). The monolayer was transferred onto the silicon surface by dipping the cleaned substrate into the trough and pulling it at a rate of 20–60 $mm\,min^{-1}$. In this way, regular line patterns with an adjustable periodicity between 300–1000 nm and a stripe/channel width ratio between 1–10 could be reproducibly obtained. The periodicity could be controlled by the transfer speed, whereas the stripe/channel width ratio was determined by the surface pressure. Chemically active structures with $-NH_2$ termination were obtained by immersing the DPPC-striped substrate into a 1 mM solution of 3-aminopropyltrimethoxysilane (APTMS, Aldrich) in 1-phenyloctane (Aldrich) for 15 min. Thereafter the polymeric residuals and DPPC stripes were removed by ultrasonication in chloroform and the silicon was cut into 20×20 mm^2 pieces. Meanwhile, a two-dimensional template with periodic stripes of aminosilane and silicon dioxide was ready for electrocrystallization. Figures 1a–d schematically illustrate the basic strategy for fabricating periodically functionalized surfaces. The experimental details are similar to those reported previously [16].

The electrodeposition was carried out in a cell with two parallel, straight electrodes made of copper foil slices (99.9 %) 40 μm thick. The electrodes were sandwiched between two rigid boundaries, one of which was a silicon wafer with a functionalized surface, and the other was a normal glass microscope slice. The separation of the electrodes was 8 mm. The electrolyte solution was prepared by analytical reagent $CuSO_4$ (Fluka) and Millipore ultrapure water. The concentration of $CuSO_4$ electrolyte was 0.07 M (pH 3.4). A schematic diagram of the experimental setup is shown in Figures 1e,f. To generate an ultrathin electrolyte layer for electrochemical deposition, we solidified the $CuSO_4$ solution by decreasing the temperature, using a Peltier element beneath the electrodeposition cell and a thermostatted circulator. Solidification started from the bottom glass plate. Meanwhile, $CuSO_4$ was partially expelled from the solid (this effect is known as the partitioning effect in crystallization [23]). As a result, the concentration of $CuSO_4$ increased in front of the ice–electrolyte interface. A very low solidification rate had to be used in order to prevent cellular interfacial morphology. On the other hand, it is known that the temperature at which an electrolyte solidifies (melting point/solidification point) depends on the concentration of electrolyte. For $CuSO_4$, the solidification temperature decreases as the salt concentration is increased. Therefore, when equilibrium was reached at a set temperature (–4.5 °C, for example), there existed an ultrathin layer of concentrated $CuSO_4$ electrolyte between the electrolyte ice and the template substrate. In our experiments, electrodeposition was carried out in this ultrathin layer, where the $CuSO_4$ concentration was expected not to exceed the saturated concentration at the setting temperature. To achieve a flat, homogeneous electrolyte–solid interface, great care should be taken at the beginning of the solidification to keep only one, or just a few, ice nuclei in the system. Several melting–solidification cycles were repeated to fulfill this requirement. The electrodeposits were observed with a field-emission SEM (LEO 1530 VP) and further analyzed with an atomic force microscope (Nanoscope IIIa) and a transmission electron microscope (FEGCM 2000).

Received: June 27, 2003
Final version: December 10, 2003

[1] a) M. Paunovic, M. Schlesinger, *Fundamentals of Electrochemical Deposition*, John Wiley & Sons, New York **1998**. b) *Modern Electro-*

plating, 4th ed., (Eds: M. Schlesinger, M. Paunovic), John Wiley & Sons, New York **2000**.
[2] Y. W. Su, C. H. Wu, C. C. Chen, C. D. Chen, *Adv. Mater.* **2003**, *15*, 49.
[3] M. P. Zach, K. H. Ng, R. M. Penner, *Science* **2000**, *290*, 2120.
[4] M. Wang, S. Zhong, X.-B. Yin, J.-M. Zho, R.-W. Peng, N.-B. Min, *Phys. Rev. Lett.* **2001**, *86*, 3827.
[5] a) Y. Xia, G. M. Whitesides, *Angew. Chem.* **1998**, *110*, 568. b) H. Sugimura, T. Hanji, K. Hayashi, O. Takai, *Adv. Mater.* **2002**, *14,* 524.
[6] *Electrochemical Technology: Innovation and New Developments* (Eds: N. Masuka, T. Osako, Y. Ito), Gordon and Breach, Amsterdam **1996**.
[7] T. A. Taton, G. L. Lu, C. A. Mirkin, *J. Am. Chem. Soc.* **2001**, *123*, 5164.
[8] J. A. Rogers, R. J. Jackmam, G. W. Whitesides, *Adv. Mater.* **1997**, *9*, 475.
[9] R. J. Jackmam, S. T Brittain, A. Adams, M. G. Prentiss, G. W. Whitesides, *Science* **1998**, *280*, 2089.
[10] S. Zhong, M. Wang, X.-B. Yin, J.-M. Zho, R.-W. Peng, N.-B. Min, *J. Phys. Soc. Jpn.* **2001**, *70*, 1452.
[11] a) C. A. Foss, M. J. Tierney, C. R. Martin, *J. Phys. Chem.* **1992**, *96*, 9001. b) S. A. Sapp, D. T. Mitchell, C. R. Martin, *Chem. Mater.* **1999**, *11*, 1183. c) C. R. Martin, *Science* **1994**, *266*, 1961.
[12] Y. C. Stephen, K. Chris, G. Jian, *Nature* **2002**, *417*, 853.
[13] K. Spratte, L. F. Chi, H. Riegler, *Europhys. Lett.* **1994**, *25*, 211.
[14] M. Gleiche, L. F. Chi, H. Fuchs, *Nature* **2000**, *403*, 173.
[15] M. Gleiche, L. F. Chi, E. Gedig, H. Fuchs, *ChemPhysChem* **2001**, *3*, 187.
[16] N. Lu, M. Gleiche, J. Zheng, S. Lenhert, B. Xu, L. F. Chi, H. Fuchs, *Adv. Mater.* **2002**, *14*, 1812.
[17] C. Leger, L. Servant, J. L. Bruneel, F. Argoul, *Physica A* **1999**, *263*, 305.
[18] V. Fleury, J. N. Chazalviel, M. Rosso, *Phys. Rev. Lett.* **1992**, *68*, 2492.
[19] F. Sagues, M. Q. Lopez-Salvans, J. Claret, *Phys. Rep.* **2000**, *337*, 97.
[20] M.-Z. Zhang, Y. Wang, S. Wang, G.-W. Yu, M. Wang, R.-W. Peng N.-B. Ming, *J. Phys.: Condens. Matter* **2004**, *16*, 695.
[21] V. V. Tsukruk, V. N. Bliznyuk, *Langmuir* **1998**, *14*, 446.
[22] P. Amirfeiz, S. Bengtsson, M. Bergh, E. Zanghellini, L. Börjessond, *J. Electrochem. Soc.* **2000**, *147*, 2693.
[23] I. V. Markov, *Crystal Growth for Beginners: Fundamentals of Nucleation, Crystal Growth and Epitaxy*, World Scientific, Singapore **1995**.

Microcontact Printing of CdS/Dendrimer Nanocomposite Patterns on Silicon Wafers**

By *Xiao C. Wu*, *Alexander M. Bittner*,* and *Klaus Kern*

Most photonics and electronics applications will eventually require parallel structuring methods for the control of the spatial positioning of functional materials, for example, multicolor LEDs, color pixels for field-emission displays, or multichannel chemical sensors. μCP is an interesting alternative to standard patterning techniques (such as lithography) due to its speed, simplicity, cheapness, and capability for high spatial resolution.[1] Patterning of functional materials via μCP is mainly based on printing passivating self-assembled monolayers (SAMs)[2] rather than the functional materials themselves. The advantage is that the interaction mechanisms between substrate, stamp, and ink (solution or suspension to cover the stamp) are well studied.[3] However, progress has recently been made in direct printing of various functional materials.[4,5] In order to achieve this a compatible stamp–material–surface system is needed. Successful printing often requires detailed studies of various printing conditions such as ink species (functional material), concentration, printing time, and surface properties of both stamp and substrate.

Nanoparticles might play an important role in future technologies such as photovoltaics, switches, phosphors, LEDs, electronic data-storage systems, and sensors.[6] Parallel schemes for positioning of these nanoparticles in fixed arrays are the basis of such potential photonic and electronic devices.[7] However, the direct patterning of these nanoparticles from solution with standard patterning techniques, such as laser ablation of the material and deposition through a shadow mask, are cumbersome, since the nanoparticles are often protected by organic surfactants (stabilizers) that tend to desorb at elevated temperature. Because the surfactants are usually necessary to stabilize the particles and to improve their functionality, any patterning approach must be carried out at low temperatures and in a mild environment.

Dendrimers are highly branched, spherically shaped molecules[8] (when the number of generations (G) is greater than four—here we employ generation-eight dendrimers). They are composed of core, repetitive unit, and terminal groups. The repetitive unit, here $-N-(CH_2CH_2-CONHCH_2CH_2-)_2$, and the terminal group, here amine, can exhibit different functionalities according to requirements. Dendrimers can be used as nanoreactors for the synthesis of various nanoparticles, such as metals, semiconductors, and magnetic oxides.[9–12] Based on dendrimer architecture, terminal groups, the loading factor of metal ions in dendrimers, and ion–ion interactions, nanoparticles can grow inside a dendrimer (internal type),[9] outside a dendrimer (external type), or in both modes.[10]

The big advantage of printing such composites is that—through the terminal groups—dendrimers can form layers on various surfaces via electrostatic forces, hydrogen bonds, van der Waals interactions, or metal–ligand interactions.[13,14] We believe that organic dendrimers will become a promising host material for the synthesis of nanoparticles and for their subsequent controlled placement on surfaces. Here, we combine the functionality of dendrimers as nanoreactors with their facile adsorption on surfaces. We demonstrate direct printing of luminescent CdS/dendrimer nanocomposites on hydroxyl-terminated silicon wafers.

We found that dendrimers can easily be transferred from hydrophilic stamps to the hydroxyl-terminated substrate.[5] Figure 1a shows polyamidoamine (PAMAM) dendrimer (gen-

[*] Dr. A. M. Bittner, Dr. X. C. Wu, Prof. K. Kern
Max-Planck-Institut für Festkörperforschung,
Heisenbergstr. 1, D-70569 Stuttgart (Germany)
E-mail: a.bittner@fkf.mpg.de

[**] We thank Dr. Christina Wege, Department of Biology, Stuttgart University for help with recording luminescence patterns.

DOI: 10.1002/adma.200306040